ELSEVIER

Contents lists available at ScienceDirect

# **Chemical Physics**

journal homepage: www.elsevier.com/locate/chemphys



# Vibrational studies of saccharide-induced lipid film reorganization at aqueous/air interfaces



Katie A. Link <sup>a</sup>, Chia-Yun Hsieh <sup>a</sup>, Aashish Tuladhar <sup>c</sup>, Zizwe Chase <sup>d</sup>, Zheming Wang <sup>c</sup>, Hongfei Wang <sup>e</sup>, Robert A. Walker <sup>a,b,\*</sup>

- <sup>a</sup> Department of Chemistry and Biochemistry, Montana State University, Bozeman, Montana, USA
- <sup>b</sup> Montana Materials Science Program, Montana State University, Bozeman, Montana, USA
- <sup>c</sup> Environmental and Molecular Sciences Laboratory, Pacific Northwest National Labs, Richland, WA, USA
- <sup>d</sup> School of Chemical and Biological Engineering, Washington State University, Pullman, WA, USA
- <sup>e</sup> Department of Chemistry, Fudan University, Shanghai, China

#### ARTICLE INFO

Article history:
Available online 9 February 2018

Keywords: Phospholipid Sum frequency generation Cooperative adsorption Isotherm Calorimetry

#### ABSTRACT

Vibrational sum frequency generation (VSFG) and surface tension experiments were used to examine the effects of aqueous phase soluble saccharides on the structure and organization of insoluble lipid monolayers adsorbed to aqueous-air interfaces. Changes in dipalmitoylphosphocholine (DPPC) chain structure as a function of aqueous phase saccharide concentration and pH are reported. Complementary differential scanning calorimetry (DSC) measurements performed on solutions containing soluble saccharides and DPPC vesicles measured the effects of the saccharides on the lipid membrane phase behavior. Data show that the saccharides glucosamine and glucuronic acid induce a higher degree of organization in compressed DPPC monolayers regardless of the saccharide's charge.

© 2018 Elsevier B.V. All rights reserved.

#### 1. Introduction

Lipid monolayers fulfill important biological and technological roles as they promote respiration in lung surfactant [1–3], inhibit ocular tear evaporation [4,5], and serve as the simplest models for understanding fluidity, permeability, and miscibility in more complex biological membranes [6–8]. Additionally, lipid monolayers have been used as media to support sensor technologies [9,10]. In each application, lipid film function depends sensitively on structure and organization within the monolayer.

Organization in lipid monolayers adsorbed to water/air interfaces depends sensitively on conditions of the aqueous sub-phase. Divalent cations such as Ca<sup>2+</sup> and Zn<sup>2+</sup> are known to induce lipid monolayer condensation [11–13], whereas small antimicrobial peptides and simple surfactants intercalate into lipid films and induce structural disorder [14–17]. Recent studies have reported that simple, soluble biomolecules also show an affinity for lipid films. Solutes such as phenylalanine [18,19] and trehalose [20] associate with lipid membranes, altering membrane permeability and phase behavior.

Recent studies have raised the prospect that solute interactions with insoluble lipid monolayers may even have meteorological

E-mail address: rawalker@montana.edu (R.A. Walker).

consequences [21]. Sea spray aerosols (SSA) nucleate ice cloud condensation with an efficacy that depends directly on SSA organic content [22]. Current descriptions of SSA composition present a paradox: data from field studies suggest that SSAs contain significantly more organic material than predicted based on the relative abundance of surface active, biogenic organic matter. In fact, the organic content of sub-micron SSA particles can reach up to 80% by mass [23–26]. To put this figure in context, a 500 nm diameter water droplet covered with a tightly packed insoluble lipid or fatty acid (e.g. stearic acid) monolayer would have an organic content of <5% by mass. The origin of observed organic enrichment in SSAs remains speculative and presents a challenge to emerging models of aerosol effects on atmospheric chemistry and climate science.

One mechanism that can account for organic enrichment in SSAs is cooperative adsorption. Cooperative adsorption describes a synergy that enhances the surface concentration of one (or more) organic species relative to expectations based on models that assume no interactions between adsorbates. This mechanism was proposed to explain SSA organic enrichment by Burrows and coworkers [21]. In that work, the authors used a Langmuir model to parameterize marine organic species partitioning into SSAs across bubble surfaces. Motivating this model was the assumption that ocean surfaces are covered (in whole or in part) with biogenic films consisting of lipids, proteins, and polysaccharides. A subsequent study used surface specific vibrational spectroscopy to determine if glucosamine (GA), a simple, soluble monosaccharide

<sup>\*</sup> Corresponding author at: Department of Chemistry and Biochemistry, Montana State University, Bozeman, Montana 59717, USA.

and the monomer unit of the biopolymer chitin, cooperatively adsorbs to tightly packed dipalmitoylphosphatidylcholine (DPPC) monolayers adsorbed to an aqueous/vapor interface [27]. Experimental data were used to infer cooperative glucosamine adsorption to the lipid monolayer through a change in solvating water structure. Fitting results to a modified Langmuir isotherm, the authors reported an effective saccharide adsorption energy of -41 kJ/mole. The authors also noted that in the absence of a lipid film, glucosamine did not show any surface affinity as evidenced by surface water structure that did not change with increasing GA concentrations up to 20 mM.

The effects of GA cooperative adsorption on DPPC monolayer organization was not addressed directly in the report by Burrows, et al. [27]. In the tightly packed monolayers studied, DPPC surface coverage was reported to be 2.5 lipids/nm<sup>2</sup> or 40 Å<sup>2</sup>/molecule with DPPC acyl chains expected to adopt highly ordered, all-trans conformations. Changes that result from cooperative adsorption to the headgroup region would not be expected to change individual chain conformation but the literature provides some evidence that soluteheadgroup interactions will affect the overall tilt of chains within insoluble lipid monolayers [11,28-31]. To further examine the viability of cooperative adsorption as a mechanism for interfacial organic enrichment, experiments described below consider cooperative adsorption of two simple monosaccharides, GA and glucuronic acid (GU), with tightly packed DPPC monolayers (40 Å<sup>2</sup>/molecule). The effects of lipid surface coverage are also examined briefly using DPPC monolayers in their liquid condensed state (55 Å<sup>2</sup>/molecule).

In this study, structure and organization in the DPPC films are monitored using vibrational sum frequency generation (VSFG) while thermodynamic changes resulting from cooperative adsorption are observed via surface tension measured with a Langmuir Trough and melting temperature measured with differential scanning calorimetry (DSC). Experiments in the tightly packed limit with GA were performed with two different aqueous phase pH conditions – 5.8 and 9.0 – with the latter pH being much closer to natural oceanic conditions (pH = 8.1). Differences in pH affect saccharide charge: GA, with a pKa of 7.58, is >98% positively charged at pH 5.8 and >96% neutral at pH 9.0, while GU, with a pKa of 3.20, is >99.6% negatively charged at pH 5.8 [32,33].

All three families of experiments - Langmuir trough, VSFG, and DSC - show evidence that glucosamine and glucuronic acid spontaneously associate with lipid films, even though the saccharides themselves are not surface active. GA and GU both induce a higher degree of order in tightly packed DPPC films on pH 5.8 solutions and, in the case of GA, this effect is more pronounced in solutions buffered to pH 9. GA also induces marked changes in VSFG intensities from DPPC films in their liquid condensed state (55 Å<sup>2</sup>/molecule) that suggest a lipid monolayer condensing effect. While this effect has been reported for divalent metal cations [11-13], spectra reported below are, to our knowledge, the first evidence that organic solutes can induce similar effects. DSC data show that both GA and GU raise the DPPC gel to liquid crystalline transition temperature, also implying saccharide-lipid association, although the effect seems much more pronounced for GU than for GA. Taken together, our data indicate that GA and GU coordinate between lipids within the film and that these interactions are driven primarily through dipolar and hydrogen bonding associations rather than Coulomb attractions.

# 2. Experimental

# 2.1. Materials

1,2-dipalmitoyl-*sn-glycero*-3-phosphocholine (DPPC, powder, >99%) was purchased from Avanti Polar Lipids Inc. (Alabaster, Alabama). D-(+)-Glucosamine hydrochloride (GA, crystalline, ≥99%),

D- Glucuronic acid (GU, powder,  $\geq$ 98%), sodium carbonate ( $\geq$ 99.5%), sodium bicarbonate ( $\geq$ 99.7%), potassium phosphate monobasic ( $\geq$ 99%), and potassium phosphate dibasic ( $\geq$ 98%) were purchased from Sigma-Aldrich (St. Louis, MO). HPLC grade chloroform (99.9%) was purchased from Fisher Scientific. All chemicals were used without further purification. Millipore water (resistivity of 18.2 M $\Omega$ ) was used for all aqueous sample preparation.

#### 2.2. Preparation of samples

DPPC stock solutions (1 mM) were prepared in HPLC grade chloroform and sonicated for 30 min. Solutions of glucosamine (GA) and glucuronic acid (GU) were prepared in Millipore water and sonicated for 30 min. Millipore solutions had a pH of 5.8. Buffer solutions at pH 9.0 (100 mM) were made with sodium carbonate and sodium bicarbonate. Buffer solutions of 6.5 and 8.5 (10 mM) were made with potassium phosphate monobasic and dibasic. Glucosamine or glucuronic acid was added to the buffer solutions before testing the pH. Solution pH plays an important role in determining speciation of the two saccharides. GA has a pKa of 7.58, meaning that in both Millipore and in the pH 6.5 buffer, the majority of GA in solution is positively charged whereas at pH 8.5, the neutral amine is the dominant species. GU, with its pKa of 3.20, is predominately negatively charged in all experiments.

To prepare samples for VSFG, the aqueous solution of interest was poured into a clean Teflon petri dish. Petri dishes were cleaned with copious amounts of methanol and Millipore water and then treated with UV/Ozone. The DPPC stock solution was spread on the surface of the aqueous solution with a glass microsyringe. After placing DPPC on the surface the sample was allowed to sit for 10 min so that the chloroform could evaporate and the DPPC monolayer could equilibrate.

# 2.3. Langmuir trough experiments

The NIMA Langmuir trough used in these experiments is a Model 302LL equipped with a PS4 pressure sensor and a Micro Processor Interface 104. The PTFE trough and barriers were wiped with chloroform on Kimwipes. Afterwards the trough and barriers were rinsed with Millipore. The surface tension of Millipore water is then measured against the standard value (72.8 mN/M at 20 °C).

The solution of interest was then added to the trough until both barriers were wetted. A paper Wilhelmy plate (Brown Waite Engineering) was then lowered into the solution. Once saturated with the bulk phase, the Wilhelmy plate was lifted out of the solution and slowly lowered until it came into contact with the surface at which point the pressure sensor was zeroed. The barriers of the trough were then closed and the surface tension was monitored. Any deviations in the surface tension were considered an impurity and the trough was then emptied, cleaned and reset. If the surface tension remained constant, the barriers were opened and a glass microsyringe was used to spread the DPPC monolayer evenly across the surface. The trough was then left to equilibrate for 10 min [34].

To collect a pressure-area isotherm, the barriers of the Langmuir trough are closed at a speed of  $10~\text{cm}^2/\text{min}$  and the surface pressure ( $\Pi$ ) is recorded as a function of surface area. The surface pressure is related to the surface tension of the neat bulk phase ( $\gamma_0$ ) and the surfactant monolayer ( $\gamma$ ) with Eq. (1).

$$\Gamma = \gamma_0 + \gamma \tag{1}$$

Pressure-area isotherms for DPPC are well reported in the literature. On Millipore water and buffered aqueous solutions, the DPPC isotherm is characterized by a liftoff pressure at  $100 \, \text{Å}^2/\text{molecule}$  and a liquid expanded/liquid condensed coexistence plateau between  $80 \, \text{Å}^2/\text{molecule}$  and  $55 \, \text{Å}^2/\text{molecule}$ . At

higher surface coverages, the DPPC isotherm rises steeply before collapsing at  $38 \, \text{Å}^2/\text{molecule}$ . Representative isotherms are shown in Fig. 1.

Two notable observations in these isotherms are that i) the distinguishing features of the DPPC 2D phase transitions are insensitive to solution pH, and ii) buffering conditions and GA, without DPPC, has no discernible effect on the surface pressure which is consistent with its high aqueous phase solubility of  $\sim\!1$  g/mL at room temperature (4.5 M). Prior spectroscopic studies showed that at concentrations up to 20 mM GA, water's surface vibrational structure was unchanged [27].

# 2.4. VSFG experiments

Sum frequency generation experiments were done at Pacific Northwest National Lab's (PNNL) EMSL facility. The details of this facility have been described in detail elsewhere [35].

Briefly, the high resolution broadband sum frequency generation vibrational spectroscopy (HR-BB-SFG-VS) system utilizes two Ti:sapphire oscillators/amplifiers. The two oscillators, a 100 ps 76 MHz TIGER (Time- Bandwidth Inc.) and sub-40 fs Micra-5 (Coherent Inc.) are electronically synchronized (Synchrolock-AP, Coherent Inc., Palo Alto, CA). The oscillators seed the two regenerative amplifiers: the Coherent Legend Elite HE-ps and the Coherent Legend Elite DUO, which produces  $\sim$ 1.6 W and  $\sim$ 7.5 W respectively. The 40 fs pulses are used to pump an optical parametric amplifier (OPerA-Solo, Coherent Inc.) to produce the IR pulse; the 100 ps pulse is used as the 800 nm source. The 800 nm visible beam and the IR beam are focused at the interface at  $45^{\circ}$  and 55°, respectively from surface normal. The sum frequency response is then isolated from the visible and IR input and collected in a monochromator (Andor Technology, Belfast, Shamrock 750 mm, 1200 lines/mm grating) and CCD (Andor Technology, Newton 971P, back-illuminated).

For surface areas of 40 Ų/molecule, 4–5 spectra, each acquired over 5 minutes, were averaged. For lower surface coverage (55 Ų/molecule), two 10-min scans were averaged. Averaged scans were background corrected with a spectrum taken with unsynchronized pulses. Spectral intensity was normalized from an averaged background subtracted SF response from a thick z-cut quartz crystal.

We note that prior measurements of the aqueous vapor interface where the aqueous phase consisted of 20 mM GA showed a

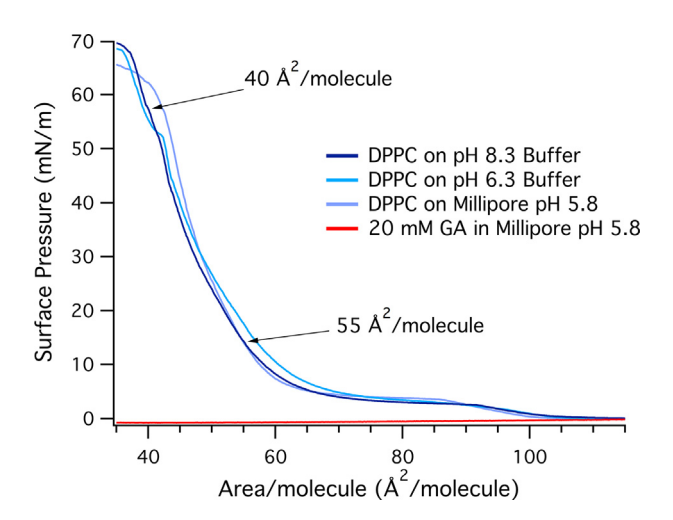


**Fig. 1.** DPPC isotherms on aqueous solutions of varying pH with no dissolved saccharide. The red/bottom trace is an 'isotherm' recorded for a 20 mM GA solution with no DPPC present. (For interpretation of the references to colour in this figure legend, the reader is referred to the web version of this article.)

distinct free –OH band at 3715 cm<sup>-1</sup> implying that GA is not surface active [27].

# 2.5. DPPC vesicle preparation and DSC measurements

Small unilamellar vesicles (SUV) were made using standard protocols [36–38]. A  $\sim$ 1 mg/mL lipid/chloroform solution was mixed in a round bottom flask. The chloroform was then removed with a rotary evaporator (>60 °C), which left behind a lipid film. The film was rehydrated with Millipore water to make a 20 mM DPPC vesicle solution. The solution was sonicated for 30 min above the melting temperature of DPPC (41 °C) to produce SUVs. Glucosamine and glucuronic acid were introduced after vesicle formation with a final DPPC concentration of 10 mM and a saccharide concentration of 50 mM. The DPPC/saccharide solutions were left to equilibrate for  $\geq$ 8 h before doing DSC measurements.

DSC measurements were performed on a TA Instruments Discovery DSC (New Castle, DE). Tzero pans and Tzero hermetic lids, purchased from TA instruments, were used as reaction vessels. First, sealed pans were equilibrated to 20 °C. Then the temperature was ramped by 0.5 °C/min until 55 °C ( $T_{\rm m}$  DPPC = 41 °C). The difference between the heat flow into the sample and the reference was recorded at each temperature interval. DSC measurements were done a minimum of 3 times with at least 2 different vesicle solutions and the reported data were the average. DSC measurements were analyzed to evaluate how saccharides affected DPPC's gel to liquid crystalline phase transition temperature ( $T_{\rm m}$ ).

#### 3. Results and discussion

# 3.1. Pressure area isotherms

This research is focused on the effects of monosaccharides on DPPC lipid monolayer structure for monolayers with two distinct surface coverages. The first coverage is 40 Å $^2$ /molecule. At this coverage, the DPPC monolayer is a 2-dimensional solid. The second coverage corresponds to 55 Å $^2$ /molecule where DPPC is in its liquid condensed phase (coverages are marked on Fig. 1).

Fig. 2 shows Langmuir isotherms for DPPC on glucosamine-containing solutions with and without a buffer. The top portion of this figure reports DPPC isotherms on unbuffered solutions with 4 GA concentrations in Millipore water. These data show little dependence on glucosamine concentration over the range sampled. The one regime where small, reproducible changes are observed occurs at high surface coverages where DPPC monolayers are more condensed with GA present. Such results are consistent with observations reported by Gobrogge, et al. where increasing concentration of GA (in Millipore water) disrupted interfacial aqueous structure—a result that was interpreted in terms of cooperative GA adsorption displacing surface water [27].

The bottom panel of Fig. 2 shows the surface pressure isotherms acquired with DPPC films adsorbed to the aqueous/vapor interface where the aqueous phase consists of a *buffered* solution containing GA. Increasing the pH with a 10 mM phosphate buffer to either 6.5 or 8.5 resulted in noticeable expansion of the lipid monolayer when GA was present in solution. The synergy between the buffer and 0.5 mM GA shifts the liquid expanded-liquid condensed coexistence plateau by  $\sim 20-25$  Ų/molecule to larger surface areas relative to DPPC on solutions containing only buffer or only GA. Such behavior is consistent with soluble solutes associated with the insoluble lipids increasing each lipid's 'effective' area per molecule. At 55 Ų/molecule, the lipid monolayer has expanded by  $\sim 9$  Ų/DPPC molecule with the addition of 0.5 mM GA and an additional  $\sim 18$  Ų/DPPC molecule with 2 mM GA. At the highest surface

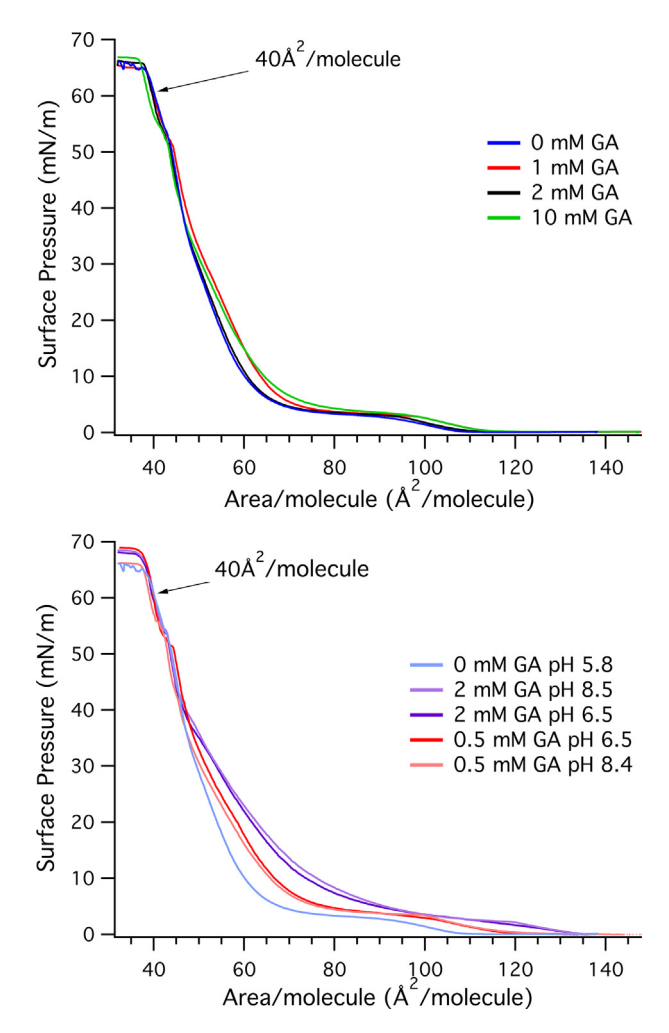


**Fig. 2.** Isotherms of DPPC monolayers on varying aqueous surfaces. Top: DPPC isotherms on solutions containing 0.0 mM to 10.0 mM GA dissolved in Millipore (pH 5.8). Bottom: DPPC isotherms on aqueous solutions (having different pH) with 0, 0.50 and 2.0 mM GA.

coverages (approaching 40  ${\rm \AA^2/DPPC}$  molecule), the isotherms converge with a common slope and collapse pressure.

The fact that such behavior is apparent only with buffer and saccharide present implies a degree of interfacial complexity and a heterogeneous distribution of species present in the interfacial region. Similar effects have been noted before (although never explored systematically) in studies examining lipid spreading across aqueous/vapor interfaces [39–42]. Clarifying and refining questions of surface composition and structure will be critical for any effort seeking to model the chemistry occurring at environmentally relevant interfaces.

# 3.2. VSFG 40 Å<sup>2</sup>/molecule DPPC on GA solutions at pH 5.8

In the two-dimensional solid phase, DPPC acyl chain organization is only modestly sensitive to changes in the underlying subphase GA concentration as evidenced by the  $-\text{CH}_3$  symmetric stretch (2870 cm $^{-1}$ , r $^*$ ) [43,44] peak intensity remaining unchanged to within experimental uncertainty as the glucosamine concentration varies between 0.0 and 10 mM and only small, systematic changes observed in the intensity of the CH<sub>2</sub> (2846 cm $^{-1}$ , d $^*$ ) symmetric stretch intensity as a function of GA concentration (Fig. 3). Nevertheless, this small change in d $^*$ 

intensity strongly affects the  $r^+$  to  $d^+$  ratio that is used frequently to infer order and organization within alkyl monolayers adsorbed to aqueous interfaces [45–47]. Under SSP polarization conditions, an increasing  $r^+/d^+$  ratio indicates an increase in acyl chain ordering within the DPPC monolayer. For the spectra shown in Fig. 3,  $r^+/d^+$  ranges from 6.0 ([GA] = 0) to 17 ([GA] = 10 mM).

Given that the acyl chains are already tightly packed in the 2-dimensional solid phase at surface coverages of  $40~\text{Å}^2/\text{molecule}$ , we propose that changes in this  $r^+/d^+$  ordering parameter may result from small changes in monolayer tilt, similar to phenomena reported in grazing incidence X-ray diffraction studies of divalent cation association with phosphocholine monolayers [29]. This hypothesis deserves further examination with alternately polarized VSFG experiments. Other symmetry allowed VSFG combinations including  $S_{\text{Sum}}P_{\text{Vis}}S_{\text{IR}}$  and  $P_{\text{Sum}}P_{\text{Vis}}P_{\text{IR}}$  probe C—H stretches having their IR transition moment aligned in the plane of the surface and can be used to determine functional group orientation. Results of these additional experiments will be the reported in future work.

# 3.3. VSFG 40 $Å^2$ /molecule DPPC on GA solutions at pH 9.0

Despite similarities in DPPC monolayer isotherms at low and high pH (Fig. 1), DPPC monolayer organization changes considerably as a function of subphase pH when GA is also present. Fig. 4 shows VSFG spectra for tightly packed DPPC monolayers (40 Å $^2$ /molecule) adsorbed to an aqueous-vapor interface with the subphase buffered to a pH of 9. In the absence of GA, the r $^+$  intensity is significantly weaker and the d $^+$  intensity is noticeably stronger than in spectra from tightly packed monolayers at pH 5.8. The DPPC r $^+$ /d $^+$  ratio under these conditions is approximately 2.

On pH 9 solutions containing increasing amounts of GA,  $r^*$  intensity rises sharply,  $d^*$  intensity diminishes, and intensity grows in the band structure centered at  $2950 \, \mathrm{cm}^{-1}$ , a region generally associated with both a  $r^*$  Fermi resonance coupling and the methyl antisymmetric stretch ( $r^-$ ). The  $r^*/d^*$  ratio reaches an asymptotic limit of  $\sim 15$ , similar to values observed for DPPC on the pH 5.8 solutions. This behavior is captured in Fig. 5 showing  $r^*/d^*$  ratios for all of the lipid/saccharide systems reported here.

With a pK<sub>a</sub> of 7.58, GA is >96% neutral in pH 9 aqueous solutions making the results shown in Fig. 4 surprising. If the small effects of

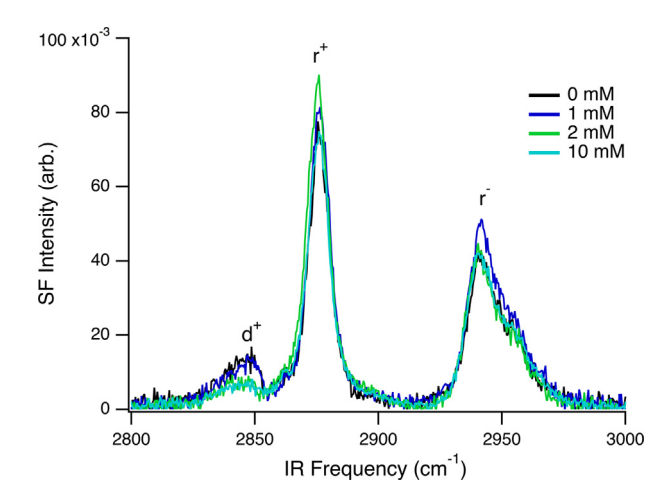


**Fig. 3.** VSF spectra (SSP polarization) of 40 Ų/molecule DPPC at the liquid/vapor interface as a function of glucosamine concentration in the subphase. Labeling conventions include a+ for a symmetric stretch and a – for an antisymmetric stretch. The d refers to a CH₂ stretch and the r to a CH₃ stretch. The r' peak intensity is compounded with signal from the  $r_{\rm FR}^{\rm c}$  ( $\sim\!2930~{\rm cm}^{-1}$ ) and the r' in and out of plane antisymmetric stretches ( $\sim\!2962~{\rm cm}^{-1}$  and  $\sim\!2952~{\rm cm}^{-1}$  respectively [43]) and are not discussed in the following analysis.

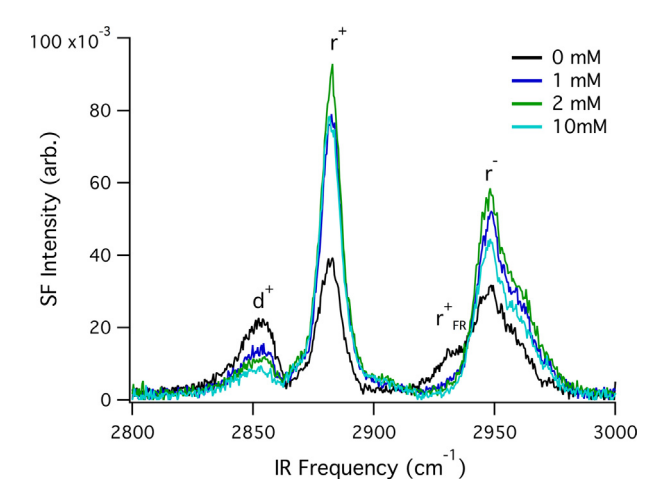


**Fig. 4.** VSF spectra (SSP polarization) of  $40 \, \text{Å}^2/\text{molecule}$  DPPC at a pH 9.0 liquid/vapor interface as a function of glucosamine concentration in the subphase.

GA on DPPC monolayer organization at pH 5.8 were due to cooperative adsorption, one might reasonably expect these interactions to be due to Coulomb attractions between the positively charged GAH $^{+}$  and the negatively charged lipid phosphate headgroup. At the higher pH, the relative amount of neutral amine (GA) and its protonated conjugate acid (GAH $^{+}$ ) has changed by a factor of  $\sim\!10^{3}$ , yet the effect of GA on the DPPC monolayer organization is just as pronounced.

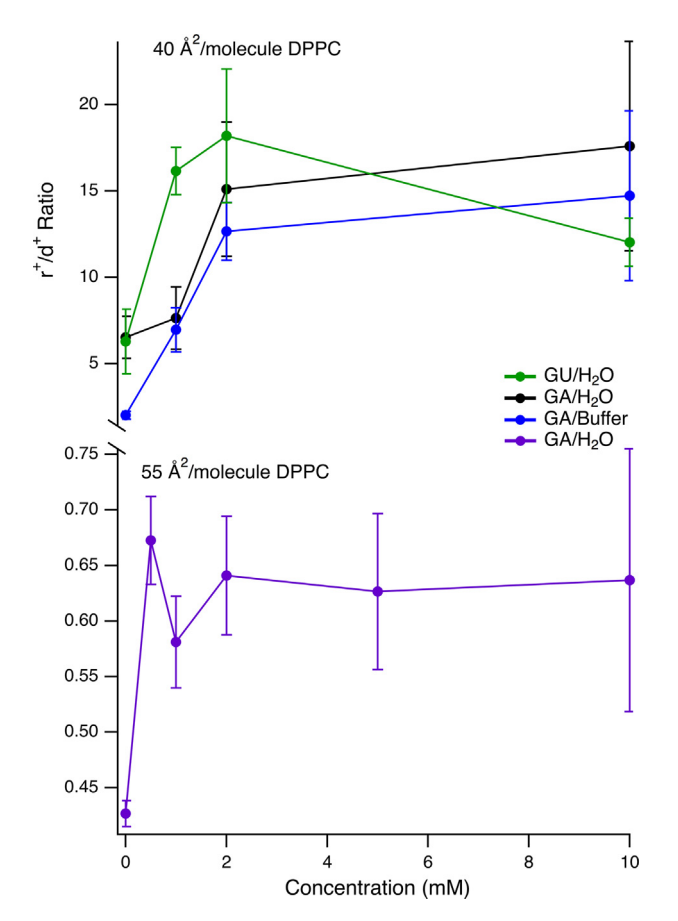


**Fig. 5.** Ratios of DPPC's  $CH_3$  symmetric stretch ( $r^*$ ) to  $CH_2$  symmetric stretch ( $d^*$ ) band intensities as a function of saccharide concentration. The top trace shows results for tightly packed (40 Ų/molecule) DPPC monolayers. The bottom trace shows data for a DPPC monolayer in its liquid condensed state (55 Ų/molecule).

# 3.4. VSFG 55 $Å^2$ /molecule DPPC on GA solutions at pH 5.8

One common denominator between VSFG spectra from tightly packed DPPC monolayers on pH 5.8 and pH 9 solutions containing GA is that the r<sup>+</sup> band is always stronger than the d<sup>+</sup> band. Such behavior is expected given that the lipid acyl chains should already be well ordered with few gauche defects. To explore this relationship further, we carried out a series of VSFG experiments on monolayers having DPPC surface coverages of 55 Å<sup>2</sup>/molecule as a function of GA concentration.

Fig. 6 shows spectra from DPPC monolayers with a surface coverage of 55  ${\mathring{A}}^2$ /molecule on solutions having different amounts of GA. Not surprisingly, monolayers with this more expanded surface coverage show considerably more acyl chain disorder than those monolayers that are tightly packed. In the absence of GA, the monolayer's  $r^+/d^+$  ratio is less than 0.45.

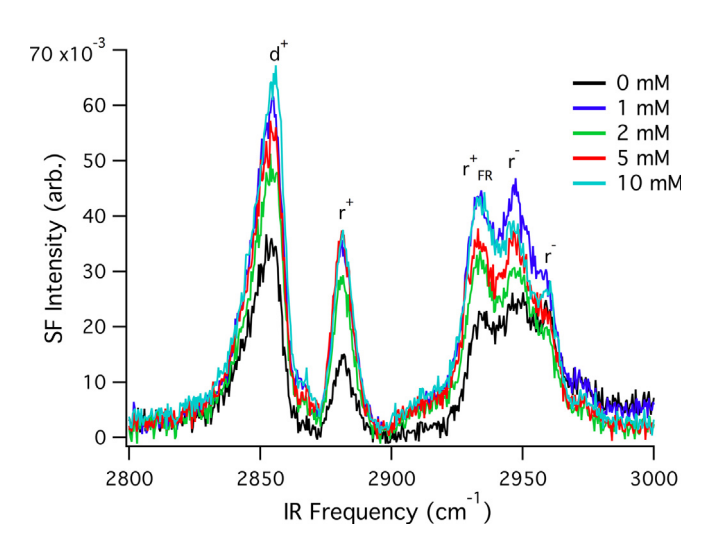
The  $d^+$  feature consistently remains stronger than  $r^+$  with increasing GA concentration, but addition of the saccharide more strongly influences the methyl symmetric stretch intensity, as evidenced by a 3-fold rise in  $r^+$  intensity and a 50% rise in the  $r^+/d^+$  ratio to 0.65 as GA concentration increases to 20 mM (Fig. 5). This behavior is consistent with GA cooperatively adsorbing to the DPPC monolayer and inducing a condensation effect as has been reported for lipid monolayers in the presence of charged, soluble alkyl surfactants [48].

# 3.5. VSFG 40 Å<sup>2</sup>/molecule DPPC on GU solutions at pH 5.8

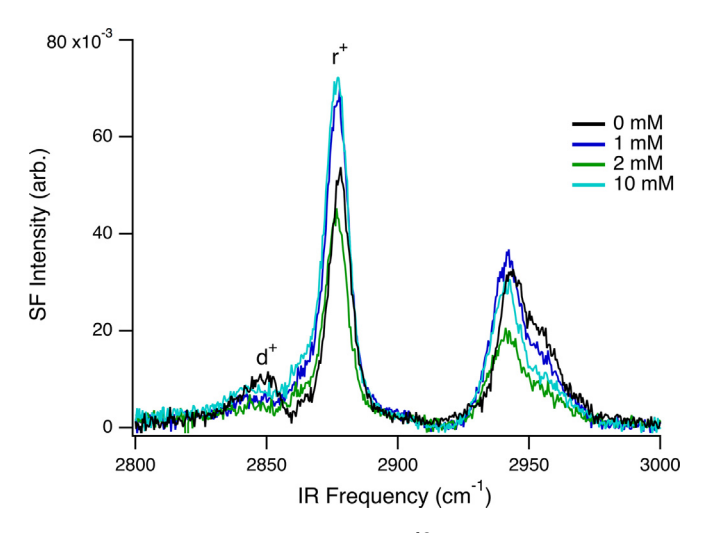
To begin examining the generality of observations made with GA, preliminary experiments were performed with a second monosaccharide, glucuronic acid (GU). Like GA, GU is a simple monosaccharide but with a carboxylic acid in the 2-position and a  $pK_a$  of 3.20. In aqueous solutions having a pH of 5.8, >95% of all GU in solution is negatively charged.

Fig. 7 shows VSFG spectra of tightly packed DPPC monolayers adsorbed to a pH 5.8 aqueous-vapor interface as a function of GU bulk concentration. Similar to the data reported for GA-containing solutions, increasing GU concentration suppresses d<sup>+</sup>.

The  $r^*/d^*$  ratios shown in Fig. 5 for the DPPC/GU system behave similarly to those observed for the DPPC/GA systems. Between GU concentrations of 2 mM and 10 mM,  $r^*/d^*$  falls from a value of 18 to 12, but given how sensitive this ratio is to small changes in the small  $d^*$  intensity, additional studies are necessary to determine whether or not this effect is real.



**Fig. 6.** VSF spectra (SSP polarization) of  $55 \text{ Å}^2/\text{molecule DPPC}$  at the liquid/vapor interface as a function of glucosamine concentration in the subphase.



**Fig. 7.** VSF spectra (SSP polarization) of 40 Å<sup>2</sup>/molecule DPPC at a pH 5.8 liquid/vapor interface as a function of glucuronic acid concentration in the subphase.

#### 3.6. DSC: Saccharide induced effect on DPPC vesicles

A final means of testing whether or not soluble monosaccharides associate with lipid films is to examine what effects these saccharides have on lipid membrane phase behavior. DSC traces of vesicles containing DPPC are shown in Fig. 8. The black trace is DPPC vesicles in Millipore with a  $T_{\rm m}$  of 40.58  $\pm$  0.02. With the addition of GA to the vesicle solution after rehydration, the  $T_{\rm m}$  of DPPC is shifted to a higher temperature by 0.25 °C. With GU present, the DPPC has 2 distinct transition temperatures. The first is shifted by 1.9 °C higher, the second by 1.02 °C from the pure DPPC.

The increase in the  $T_m$  with the addition of either GA or GU indicates saccharide association with the lipid vesicles. The two-endotherm behavior in the DPPC/GU trace is consistent with previous reports of dehydration of a DPPC bilayer. Kodama *et al.* reported that a decrease in water content from 80 wt% to 47 wt% resulted in another endotherm appearing as a shoulder of the original isotherm, but shifted to a higher temperature [49]. This behavior mirrors the effects that GU has on DPPC membrane behavior in vesicles. Specifically, the second transition temperature suggests that negative GU ions are displacing solvating water surrounding the DPPC headgroups. If true, this behavior is interesting in that

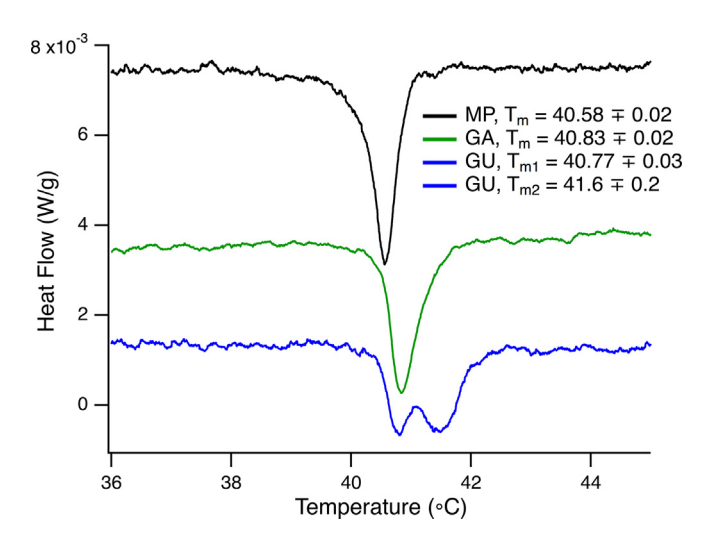


Fig. 8. Calorimetric traces of DPPC vesicles in saccharide containing solutions.

the dehydration of DPPC monolayers and vesicles is normally attributed to cation, not anion, effects on charged ions [50].

The incorporation of GU into the vesicle structure as replacement for water lends evidence to a cooperatively between GU and the positively charged  $3^\prime$  amine group. The association of GAH<sup>+</sup>(causing the shift to higher  $T_m$ ) to the negatively charged phosphate group of the DPPC has less of a dehydration effect than the presumed GU<sup>-</sup> association with the positively charged quaternary ammonium headgroup, suggesting that negatively charged associations to lipid structures may be more impactful than previous studies have assumed.

#### 4. Conclusions

Experimental studies described in this work broadly surveyed the effects of soluble monosaccharides on the organization and phase behavior of DPPC films. Specifically, surface tension isotherms showed that while saccharides modestly alter DPPC monolayer formation, saccharides and buffer constituents expand the monolayer and induce significant reorganization that is apparent in changes of vibrational band intensities. For the conditions sampled in these experiments, synergy between the soluble saccharide and the lipid film effect does not correlate with pH but rather the amount of saccharide present. DSC data also suggest measurable association between monosaccharides in solution and the DPPC membranes in vesicle bilayers. Together, these results add plausibility to the hypothesis that cooperative adsorption can enhance the organic content of aqueous/vapor interfaces in environmentally relevant systems.

# Acknowledgements

The SFG measurements were performed at the William R. Wiley Environmental Molecular Science Laboratory (EMSL), a national scientific user facility sponsored by the U.S. Department of Energy's Office of Biological and Environmental Research and located at the Pacific Northwest National Laboratory, operated for the Department of Energy by Battelle. (EMSL user proposal 48281) The authors also acknowledge support from the Montana Research and Economic Development Initiative (M-REDI) and the National Science Foundation (CHE-1710695). The authors declare no competing financial interests.

# References

- [1] H. Zhang, Q.H. Fan, Y.E. Wang, C.R. Neal, Y.Y. Zuo, Comparative study of clinical pulmonary surfactants using atomic force microscopy, Biochimica Et Biophysica Acta-Biomembranes 2011 (1808) 1832–1842.
- [2] G. Ma, H.C. Allen, New insights into lung surfactant monolayers using vibrational sum frequency generation spectroscopy, Photochem. Photobiol. 82 (2006) 1517–1529.
- [3] K. Nag, J. Perez-Gil, M.L.F. Ruano, L.A.D. Worthman, J. Stewart, C. Casals, K.M.W. Keough, Phase transitions in films of lung surfactant at the air-water interface, Biophys. J. 74 (1998) 2983–2995.
- [4] P. Kulovesi, J. Telenius, A. Koivuniemi, G. Brezesinski, I. Vattulainen, J.M. Holopainen, The impact of lipid composition on the stability of the tear fluid lipid layer, Soft Matter. 8 (2012) 5826–5834.
- [5] W. Mathers, Evaporation from the ocular surface, Exp. Eye Res. 78 (2004) 389-
- [6] A.L. Plant, Supported hybrid bilayer membranes as rugged cell membrane mimics, Langmuir 15 (1999) 5128–5135.
- [7] E. Sackmann, Supported membranes: scientific and practical applications, Science 271 (1996) 43–48.
- [8] G. Ma, H.C. Allen, DPPC Langmuir monolayer at the air-water interface: Probing the tail and head groups by vibrational sum frequency generation spectroscopy, Langmuir 22 (2006) 5341–5349.
- [9] M.A. Borden, M.L. Longo, Oxygen permeability of fully condensed lipid monolayers, J. Phys. Chem. B 108 (2004) 6009–6016.
- [10] F.A. Scholl, P.V. Morais, R.C. Gabriel, M.J. Schoning, J.R. Siqueira, L. Caseli, Carbon Nanotubes Arranged As Smart Interfaces in Lipid Langmuir-Blodgett Films Enhancing the Enzymatic Properties of Penicillinase for Biosensing Applications, Acs Appl. Mater. Interfaces 9 (2017) 31054–31066.

- [11] E.M. Adams, C.B. Casper, H.C. Allen, Effect of cation enrichment on dipalmitoylphosphatidylcholine (DPPC) monolayers at the air-water interface, J. Colloid Interface Sci. 478 (2016) 353–364.
- [12] E.M. Adams, D. Verreault, T. Jayarathne, R.E. Cochran, E.A. Stone, H.C. Allen, Surface organization of a DPPC monolayer on concentrated SrCl2 and ZnCl2 solutions, PCCP 18 (2016) 32345–32357.
- [13] N. Kucerka, E. Dushanov, K.T. Kholmurodov, J. Katsaras, D. Uhrikova, Calcium and zinc differentially affect the structure of lipid membranes, Langmuir 33 (2017) 3134–3141.
- [14] D. Ciumac, R.A. Campbell, H. Xu, L.A. Clifton, A.V. Hughes, J.R.P. Webster, J.R. Lu, Implications of lipid monolayer charge characteristics on their selective interactions with a short antimicrobial peptide, Colloids Surf. B-Biointerfaces 150 (2017) 308–316.
- [15] N. Joondan, S. Jhaumeer-Laulloo, P. Caumul, Effect of Chain Length on the Micellization, Antibacterial, DPPC Interaction and Antioxidant Activities of L-3,4-Dihydroxyphenylalanine (L-DOPA) Esters, J. Surfactants Deterg. 18 (2015) 1095–1104.
- [16] M.A. Mendez, Z. Nazemi, I. Uyanik, Y. Lu, H.H. Girault, Melittin adsorption and lipid monolayer disruption at liquid-liquid interfaces, Langmuir 27 (2011) 13918–13924.
- [17] L.C. Salay, M. Ferreira, O.N. Oliveira, C.R. Nakaie, S. Schreier, Headgroup specificity for the interaction of the antimicrobial peptide tritrpticin with phospholipid Langmuir monolayers, Colloids Surf. B-Biointerfaces 100 (2012) 95–102
- [18] E.C. Griffith, R.J. Perkins, D.M. Telesford, E.M. Adams, L. Cwiklik, H.C. Allen, M. Roeseova, V. Vaida, Interaction of L-Phenylalanine with a Phospholipid Monolayer at the Water-Air Interface, J. Phys. Chem. B 119 (2015) 9038–9048.
- [19] R. Perkins, V. Vaida, Phenylalanine Increases Membrane Permeability, J. Am. Chem. Soc. 139 (2017) 14388–14391.
- [20] M. Doxastakis, A.K. Sum, J.J. de Pablo, Modulating membrane properties: the effect of trehalose and cholesterol on a phospholipid bilayer, J. Phys. Chem. B 109 (2005) 24173–24181.
- [21] S.M. Burrows, O. Ogunro, A.A. Frossard, L.M. Russell, P.J. Rasch, S.M. Elliott, A physically based framework for modeling the organic fractionation of sea spray aerosol from bubble film Langmuir equilibria, Atmos. Chem. Phys. 14 (2014) 13601–13629.
- [22] T.W. Wilson, L.A. Ladino, P.A. Alpert, M.N. Breckels, I.M. Brooks, J. Browse, S.M. Burrows, K.S. Carslaw, J.A. Huffman, C. Judd, W.P. Kilthau, R.H. Mason, G. McFiggans, L.A. Miller, J.J. Najera, E. Polishchuk, S. Rae, C.L. Schiller, M. Si, J.V. Temprado, T.F. Whale, J.P.S. Wong, O. Wurl, J.D. Yakobi-Hancock, J.P.D. Abbatt, J.Y. Aller, A.K. Bertram, D.A. Knopf, B.J. Murray, A marine biogenic source of atmospheric ice-nucleating particles, Nature 525 (2015) 234-+.
- [23] J.Y. Aller, J.C. Radway, W.P. Kilthau, D.W. Bothe, T.W. Wilson, R.D. Vaillancourt, P.K. Quinn, D.J. Coffman, B.J. Murray, D.A. Knopf, Size-resolved characterization of the polysaccharidic and proteinaceous components of sea spray aerosol, Atmos. Environ. 154 (2017) 331–347.
- [24] A.P. Ault, R.C. Moffet, J. Baltrusaitis, D.B. Collins, M.J. Ruppel, L.A. Cuadra-Rodriguez, D.F. Zhao, T.L. Guasco, C.J. Ebben, F.M. Geiger, T.H. Bertram, K.A. Prather, V.H. Grassian, Size-Dependent Changes in Sea Spray Aerosol Composition and Properties with Different Seawater Conditions, Environ. Sci. Technol. 47 (2013) 5603–5612.
- [25] C.D. O'Dowd, G. De Leeuw, Marine aerosol production: a review of the current knowledge, Philos. Trans. R. Soc. a-Math. Phys. Eng. Sci. 365 (2007) 1753– 1774.
- [26] P.K. Quinn, T.S. Bates, K.S. Schulz, D.J. Coffman, A.A. Frossard, L.M. Russell, W.C. Keene, D.J. Kieber, Contribution of sea surface carbon pool to organic matter enrichment in sea spray aerosol, Nat. Geosci. 7 (2014) 228–232.
- [27] S.M. Burrows, E. Gobrogge, L. Fu, K. Link, S.M. Elliott, H.F. Wang, R. Walker, OCEANFILMS-2: representing coadsorption of saccharides in marine films and potential impacts on modeled marine aerosol chemistry, Geophys. Res. Lett. 43 (2016) 8306–8313
- [28] U.M. Ferber, G. Kaggwa, S.P. Jarvis, Direct Imaging of Salt Effects on Lipid Bilayer Ordering at Sub-molecular Resolution, Eur. Biophys. J. Biophys. Lett. 40 (2011) 329–338.

- [29] S.K. Ghosh, S. Castorph, O. Konovalov, T. Salditt, R. Jahn, M. Holt, Measuring Ca2+ Induced Structural Changes in Lipid Monolayers: Implications for Synaptic Vesicle Exocytosis, Biophys. J. 102 (2012) 1394–1402.
- [30] S. Kewalramani, H. Hlaing, B.M. Ocko, I. Kuzmenko, M. Fukoto, Effects of Divalent Cations on Phase Behavior and Structure of a Zwitterionic Phosphlipid (DMPC) Monolayer at the Air-Water Interface, J. Phys. Chem. Lett. 1 (2010) 489–495.
- [31] W. Lin, A.J. Clark, F. Paesani, Effects of surface pressure on the properties of Langmuir monolayers and interfacial water at model sea spray aerosol surfaces, Langmuir 31 (2015) 2147–2156.
- [32] Y. Bichsel, U. vonGunten, Formation of iodo-trihalomethanes during disinfection and oxidation of iodide containing waters, Environ. Sci. Technol. 34 (2000) 2784–2791.
- [33] J.S. Rohrer, Applications of Ion Chromatography for Parmaceutical and Biological Products, 1st ed., John Wiley and Sons, Inc., 2012.
- [34] M.S. Aston, The Study of Surfactant Monolayers by Surface Pressure Area Measurement, Chem. Soc. Rev. 22 (1993) 67–71.
- [35] L. Velarde, H.F. Wang, Capturing inhomogeneous broadening of the -CN stretch vibration in a Langmuir monolayer with high-resolution spectra and ultrafast vibrational dynamics in sum-frequency generation vibrational spectroscopy (SFG-VS), J. Chem. Phys. 139 (2013), 084204.
   [36] C.A. Gobrogge, H.S. Blanchard, R.A. Walker, Temperature-Dependent
- [36] C.A. Gobrogge, H.S. Blanchard, R.A. Walker, Temperature-Dependent Partitioning of Coumarin 152 in Phosphatidylcholine Lipid Bilayers, J. Phys. Chem. B 121 (2017) 4061–4070.
- [37] C.A. Gobrogge, R.A. Walker, Quantifying Solute Partitioning in Phosphatidylcholine Membranes, Anal. Chem. 89 (2017) 12587–12595.
- [38] Avanti\_Polar\_Lipids, Liposome Preparation, 2017.
- [39] M. Kozak, L. Domka, S. Jurga, Interactions of cationic surfactantswith DPPC, J. Therm. Anal. Calorim. 88 (2007) 395–399.
- [40] H.M. Mansour, G. Zografi, Relationships between equilibrium spreading pressure and phase equilibria of phospholipid bilayers and monolayers at the air-water interface, Langmuir 23 (2007) 3809–3819.
- [41] C.W. McConlogue, D. Malamud, T.K. Vanderlick, Interaction of DPPC monolayers with soluble surfactants: electrostatic effects of membrane perturbants, Biochimica Et Biophysica Acta-Biomembranes 1372 (1998) 124-134.
- [42] G.A. Clark, J.M. Henderson, C. Heffern, B. Akgün, J. Majewski, K.Y.C. Lee, Synergistic Interactions of Sugars/Polyols and Monovalent Salts with Phospholipids Depend upon Sugar/Polyol Complexity and Anion Identity, Langmuir 31 (2015) 12688–12698.
- [43] R.A. Macphail, H.L. Strauss, R.G. Snyder, C.A. Elliger, C.-H. Stretching, Modes and the Structure of Normal Alkyl Chains. 2. Long, All-trans Chains, J. Phys. Chem. 88 (1984) 334–341.
- [44] R.G. Snyder, H.L. Strauss, C.A. Elliger, C.-H. Stretching, Modes and the Structure of Normal Alkyl Chains. 1. Long Disordered Chains, J. Phys. Chem. 86 (1982) 5145–5150.
- [45] S.Z. Can, D.D. Mago, R.A. Walker, Structure and organization of hexadecanol isomers adsorbed to the air/water interface, Langmuir 22 (2006) 8043–8049.
- [46] R.A. Walker, J.A. Gruetzmacher, G.L. Richmond, Phosphatidylcholine monolayer structure at a liquid-liquid interface, J. Am. Chem. Soc. 120 (1998) 6991–7003.
- [47] S. Ye, M. Osawa, Molecular Structures on Solid Substrates Probed by Sum Frequency Generation (SFG) Vibration Spectroscopy, Chem. Lett. 38 (2009) 386–391.
- [48] S.Z. Can, C.F. Chang, R.A. Walker, Spontaneous formation of DPPC monolayers at aqueous/vapor interfaces and the impact of charged surfactants, Biochimica Et Biophysica Acta-Biomembranes 1778 (2008) 2368–2377.
- [49] M. Kodama, M. Kuwabara, S. Seki, Successive phase-transition phenomena and phase diagram of the phosphatidylcholine-water system as revealed by differential scanning calorimetry, Biochimica et Biophysica Acta (BBA) Biomembranes 689 (1982) 567–570.
- [50] H. Minami, T. Inoue, Dehydration of Hydrated Bilayer of Dipalmitoylphosphatidylcholine caused by Beryllium Ion: Evidence from a Differential Scanning Calorimetry of Bilayer Phase Transition, J. Colloid Interface Sci. 206 (1998) 338–341.